A high-throughput microfluidic device to study neurite response to growth factor gradients

Chandrasekhar R. Kothapalli, Ed van Veen, Sarra de Valence, Seok Chung, Ioannis K. Zervantonakis, Frank B. Gertler, Roger D. Kamm

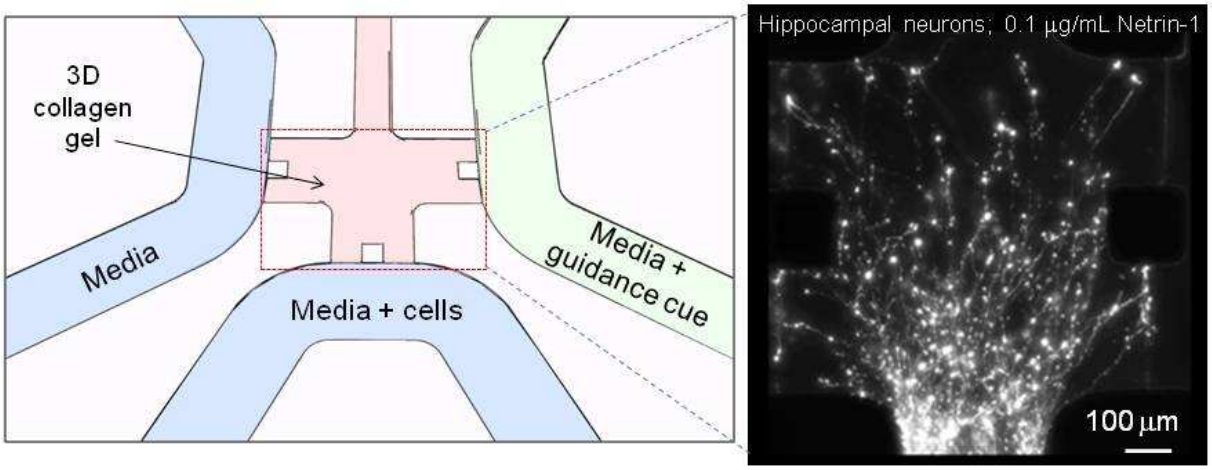

Growth factor gradients have been implicated in many biological phenomena, including cell migration, neurite outgrowth and guidance in the nervous system. Current in vitro assays to study the effect of growth factors on neurite guidance are limited by their suitability for only substrate-bound gradients and 2D cultures. Here we describe a novel three-channel microfluidic device to study the role of chemogradients on neurite outgrowth and guidance in 3D scaffolds. Neurons packed in the bottom channel onto the collagen gel surface extended their neurites into the gel in three dimensions, and the growing neurites were exposed to a chemogradient orthogonal to the direction of their growth to quantify their response and turning. Experimental and computational studies showed that a linear stable chemogradient could be established in these devices within 30 min, and lasting for up to 48 h. Cell culture studies revealed the dramatic effect of chemoattractive (netrin-1, brain pulp) and chemorepulsive (slit-2) gradients on the migration and neurite guidance of hippocampal and dorsal root ganglion neurons cultured in these devices. The stable chemogradients in these 3-channel devices could not only be used to screen potential drugs suitable for neuron pathway regeneration under disease/ injury conditions, but also to study cancer cell migration and cell-cell interactions.

A high-throughput microfluidic assay to study neurite response to growth factor gradients

Chandrasekhar R. Kothapalli[1], Ed van Veen[2,‡], Sarra de Valence[1,‡], Seok Chung[4], Ioannis K. Zervantonakis[3], Frank B. Gertler[2], Roger D. Kamm[1, 3, 5]

[1]Department of Biological Engineering, Massachusetts Institute of Technology, Cambridge, MA 02139, USA

[2]Department of Biology, Massachusetts Institute of Technology, Cambridge, MA 02139, USA

[3]Department of Mechanical Engineering, Massachusetts Institute of Technology, Cambridge, MA 02139, USA

[4]School of Mechanical Engineering, Korea University, Seoul, Korea

[5]Corresponding author: rdkamm@mit.edu

‡ equally contributing second authors

Abstract

Studying neurite guidance by diffusible or substrate bound gradients is challenging with current techniques. In this study, we present the design, fabrication and utility of a microfluidic device to study neurite guidance under chemogradients. Experimental and computational studies demonstrated the establishment of a steep gradient of guidance cue within 30 min and stable for up to 48 h. The gradient was found to be insensitive to external perturbations such as media change and movement of device. The effects of netrin-1 (0.1-10 μg/mL) and brain pulp (0.1 μL/mL) were evaluated for their chemoattractive potential on neurite turning, while slit-2 (62.5 or 250 ng/mL) was studied for its chemorepellant properties. Hippocampal or dorsal root ganglion (DRG) neurons were seeded into a micro-channel and packed onto the surface of a 3D collagen gel. Neurites grew into the matrix in three dimensions, and a gradient of guidance cue was created orthogonal to the direction of neurite growth to impact guidance. The average turning angle of each neurite was measured and averaged across multiple devices cultured under similar conditions to quantify the effect of guidance cue gradient. Significant positive turning towards gradient were measured in the presence of brain pulp and netrin-1 (1 μg/mL), relative to control cultures which received no external guidance cue ($p < 0.001$). Netrin-1 released from transfected fibroblasts had the most positive turning effect of all the chemoattractive cues tested (p

< 0.001). Slit-2 exhibited strong chemorepellant characteristics on both hippocampal and DRG neurite guidance at 250 ng/mL concentration. Slit-2 also showed similar behavior on DRG neuron invasion into 3D collagen gel ($p < 0.01$ relative to control cultures). Taken together, the results suggest the utility of this microfluidic device to generate stable chemogradients for studying neurobiology, cell migration and proliferation, matrix remodeling and co-cultures with other cell lines, with potential applications in cancer biology, tissue engineering and regenerative medicine.

Key Words: Microfluidics, neurite turning, netrin-1, 3D culture, chemogradients, slit-2

Introduction

During nervous system development, a tightly-regulated complex neural network is established by spatio-temporal regulation of guidance molecules that direct the growth of neurites along specific pathways to reach the target[1]. This process depends on the chemoaffinity of growth cones (the tip of the neurite) to sense and respond to multiple attractive and repulsive guidance cues operating at different length scales in the environment[2]. However, the precision and mechanism by which the distribution of guidance cues is maintained within the nervous system are not clear yet. Earlier studies have shown that neurites fail to regenerate and accurately reestablish the lost neuronal network connections after an injury to the central nervous system[3]. Although numerous tissue engineering strategies have been explored to promote neurite regeneration at the site of injury[4], successful practical realization of these approaches is contingent upon elucidating the effects of concentration and gradient of developmentally

important guidance cues on neurite response and turning, especially in the inflammatory environment at the injury site.

Growth factor gradients have been implicated in many biological phenomena, including cell migration, neurite outgrowth and guidance in the nervous system[5]. It is now generally accepted that neurite outgrowth and guidance is controlled by the concerted action of attractive and repulsive cues, arranged in substrate-bound and diffusible gradients, to facilitate tunneling through the tissue and connecting to distant targets[6]. Although *in vivo* studies on neurite guidance are very powerful in identifying cues relevant to neural development, it is impossible to control the microenvironment around the neurons, and evaluate the role of the multitude of cues to which the growth cones are exposed. Thus, researchers have developed numerous experimental and computational techniques to study the effects of growth factors on neurite outgrowth *in vitro*. In one technique, neural tissue explants embedded in collagen matrix are exposed to a source of guidance cue released from transfected cells[7], microbeads[8], or diffusible micropatterned gradients on collagen gel surface[9]. Quantification in these assays was limited to comparing neurite outgrowth from the explants on the higher and lower concentration sides. While these methods have been successful in identifying the global response of neuronal population to a specific cue, they generally fail to distinguish the effect of biomolecular gradients on neurite outgrowth and guidance. Moreover, it is difficult to trace individual neurites as they grow out of the explant, due to their dense overlap on 2-dimensional coated surfaces. In other *in vitro* assays, discontinuous[10] or continuous[11] gradients of guidance cues are printed onto the surface,

on which the neurons are cultured and neurite growth observed. However, limitations of this technique include its suitability for only substrate-bound gradients and 2D cultures.

Micropipette turning assays have commonly been used for studying neurite guidance *in vitro*[12]. Here, the micropipette serves as a continuous point source of chemoattractant, producing a growth factor gradient by diffusion to guide neurite growth[13, 14]. However, the gradient produced by localized factor delivery is spatially non-uniform, and varies significantly with the molecular weight of diffusible cue, height of micropipette tip, and the pulse duration and frequency. In all the above assays, the gradients generated by these traditional methods are unstable, difficult to quantify and often lack defined spatio-temporal control. To elucidate the complexities of physiologically-relevant growth factor gradients and their specific cell signaling processes, user-defined control over the spatio-temporal distribution of growth factor in the extracellular matrix environment and the ability to directly visualize cells within that environment is essential.

Over the past decade, microfluidic devices have gained popularity in cell culture applications, because they offer a great platform for studying how cells respond to alterations of their physical and chemical milieu[15,16,17]. These devices are also useful for creating well-defined 2D and 3D cell culture environments with micrometer precision, quantifiable characterization and experimental reproducibility. Microfluidic devices with simple geometries were also developed to demonstrate the effect of mechanical constraints on axon growth[18], though axonal turning and guidance could not be studied in these devices. Similarly microfluidic gradient mixers were developed to study the effects of substrate-bound gradients on neuron survival and outgrowth[19]. Since neurons

are sensitive to shear stress[20], these gradient-generating devices may not be suitable to study the effect of diffusible cues on neurite turning. In this context, devices employing surface gradients of substrate cues[21] or microgroove based devices might be more effective in isolating neurites from their cell bodies and studying their outgrowth and turning[22,23]. It can be seen from these earlier studies that stable biomolecular gradients can be created in microfluidic devices for studying neurite guidance by diffusible growth factors, although no such microfluidic system exists yet.

In this study, we present a novel microfluidic system to study neurite guidance by diffusible factors in a 3D *in vitro* cell culture model. Neurons cultured in this device extend neurites in a 3D physiological configuration, and then the growing neurites are exposed to guidance cue gradients orthogonal to the direction of neurite growth, making it an effective technique to study their guidance. We demonstrate the utility of this device to study the effects of various chemoattractive/ repulsive guidance cues, their mode of delivery and variable concentration gradients, on hippocampal and DRG neurite outgrowth and turning. This system can also be used to study other neuronal cell types, either as single cultures or co-cultures. We believe that this device has strong potential for applications at the interface of neuroscience, developmental cell biology, advanced biomaterials and microfluidic technology.

Materials and methods

Microfluidic device: design and fabrication

The microfluidic device was fabricated using photolithography and soft-lithography techniques described in detail elsewhere[24]. As shown in Fig. 1, the device design was created in AutoCAD (Autodesk, San Rafael, CA) and a transparency mask was created from the CAD file and printed by a high-resolution printer (PageWorks, MA). The silicon wafer was first spin-coated with a SU-8 photoresist at a thickness of 120 μm. A transparency mask printed with the negative pattern of the device was placed over the wafer and exposed to UV-light, which crosslinked the photoresist in the exposed areas. The uncrosslinked photoresist was then washed away, resulting in a silicon wafer layered with the positive relief of the device. Microfluidic devices were made by replica molding[25] polydimethylsiloxane (PDMS; Dow Corning, USA) and curing the degassed elastomer mix (10:1, base: curing agent) against the silicon master in an 80 ℃ oven for 2.5 h. Polymerized PDMS devices were peeled off the silicon master, individual devices (30 mm diameter, 1 cm height) cut out and inlets and outlets cored down to microfluidic channels using standard 4 mm and 1 mm diameter punching tools. Prior to cell culture, PDMS devices were air-dusted, washed multiple times in DI water, autoclaved at 120 ℃ for 35 min (20 min sterilization/ 15 min dry), soaked in ethanol for 2 h and dried overnight to remove debris and sterilize the devices. The glass cover-slips were air-dusted and autoclaved for 30 min (dry). PDMS surface and cover-slips were oxidized by air plasma for 45 sec, before they were bonded together, closing the channels and completing the device fabrication. This surface treatment ensures an irreversible bond between PDMS and cover-slip and also helps in preventing leaks. To restore hydrophobicity before filling the gel scaffold, the devices were kept at 80 ℃ overnight.

Collagen gel loading in PDMS devices

Sterilized PDMS wafers with their surfaces rendered hydrophobic (as described above) were filled with 2 mg/mL collagen type I isolated from rat tail (BD Biosciences, San Jose, CA; stored at 4 ℃). Collagen solution was prepared by adding collagen stock solution to a mixture of 10 X PBS, 1 M NaOH and tissue culture grade water to obtain a 2 mg/mL solution at pH 7.4. A cold pipette tip pre-loaded with 2 μL of collagen gel solution was carefully lowered into the gel-loading port of the device, and ice cold gel was microinjected into the device until the designated gel-region within the micro-pillars was filled (Fig. 1). This process was repeated in multiple devices for each experimental condition. After gel injection, PDMS wafers were placed in a humidified container to prevent the hydrogels from drying out, and the gels were allowed to polymerize for 30 min at 37 ℃ in a humidified incubator. The gel was filled 24 h prior to experiment and left in the incubator to allow any air bubbles in the microchannels to resorb.

Gradient simulation and visualization

Following collagen gel polymerization, microfluidic channels were filled with cell culture media. Gradient studies were performed under static conditions with the media in chemoattractant channel (Fig. 1) replaced by a dilute solution of florescent FITC-dextran (40 kDa, Invitrogen, CA) at an initial concentration of 10 μM (Fig. 2). Since netrin-1 has been reported not to bind to collagen type I[26], usage of a Dextran molecule which also does not bind to collagen type I gel is relevant. The other channels were filled with serum-free media. Florescent intensity was captured with a Nikon TE300 fluorescent

microscope (Nikon Instruments Inc., NY, USA). A series of florescent images of the gel region were acquired every 5 min for the first half hour and then every half hour for 3-5 h, with a Hamamatsu camera (Hamamatsu, Shizuoka, Japan) using Openlab (Improvision, Waltham, MA) data acquisition software. The device was then brought to the incubator to prevent excess drying of the media, and further images were taken at 6 h intervals by stabilizing the device on a microscope stand for 30 min before acquiring the images. Image processing of time-lapse florescent images was performed using a custom written code in MATLAB (MathWorks, Natick, MA), to obtain the changes in florescent intensity across the gel at each time point. Briefly, pixel values were normalized by subtracting the background intensity value, and then divided by the maximum pixel value of 10 μM Dextran. The diffusion profiles were analyzed by averaging a horizontal rectangle along the gel region and plotted against its position in the channel (Fig. 2B insert). Each image was normalized with the maximum and minimum obtained from the first image of the series.

A diffusion-convection-reaction finite element model was developed in COMSOL (Burlington, MA) for quantifying concentration gradients under different experimental conditions and performing parametric analyses. Constant concentration boundary conditions were defined at the numerical model boundaries, for representing source conditions at the inlet (C_{SOURCE}) and sink conditions at the outlet (C_{SINK}) of the control channel and at the gel filling port. For the transient simulations, the initial concentration in the condition channel was set equal to that of the inlet to simulate the characterization experiments. Based on the experimental characteristics, we defined a diffusion coefficient of $D_{GEL} = 5.1 \times 10^{-11}$ m^2/s for the growth-factor diffusion inside the collagen

matrix, which agrees with the reported values of Helm et al.,[27] for 2 mg/mL collagen gels. The diffusion coefficient inside the medium-containing channels was set to $D_M = 6 \times 10^{-11}$ m^2/s, according the Stokes-Einstein relationship for a 40 kDa molecular weight protein. The numerical grid for performing the simulations consisted of approximately 400,000 finite elements.

Neuron isolation and culture

Primary hippocampal neurons and dorsal root ganglion (DRG) neurons cultured in the devices were obtained from embryonic day 14.5-16.5 mice as per protocols described in detail elsewhere[28, 29, 30]. Cells from micro-dissected cortices were dissociated and resuspended in serum-free media at a final concentration of 10 million cells/mL. The neurons were seeded into the devices (n = 10 devices per test condition) immediately after dissociation and cultured for 1-2 days, with serum-free media replaced in all the channels twice a day, before any guidance cue was introduced. All cell cultures were maintained in a humidified incubator at 5% CO_2 and 37 °C. For netrin-1 studies (Fig. 6 A-C), hippocampal neurons were transfected using amaxa nucleofection, with a pmax-gfp plasmid co-transfected with a plasmid expressing DCC (deleted in colorectal cancer) receptor[31].

Guidance cue addition and media change

Netrin-1 added in the channel was obtained from multiple sources: lab-isolated[32] netrin-1 (0.1-10 μg/mL), and netrin-1 released from cDNA transfected stable fibroblast cell line[33]. Commercially obtained netrin-1 at 0.1 μg/mL (R&D Systems, Minneapolis, MN) was also tested under similar culture conditions, but did not provide any additional advantage compared to that of lab-purified netrin-1 (data not shown). Brain pulp was prepared in the lab from fresh whole mouse brain tissues. Briefly, the brain tissue was homogenized with a rotor stator in a hypotonic solution supplemented with protease inhibitors (protease inhibitor cocktail; Roche, USA), filtered, total protein content measured using a Bradford protein assay, and diluted to 0.1 μL/mL concentration. The chemorepellant used was Slit-2 (62.5 or 250 ng/mL; R&D Systems, Minneapolis, MN)). For chemosensing studies, the medium was removed from all the ports after 24-48 h of cell seeding, and 350 μL medium containing known concentration of guidance cue was introduced in the chemoattractant channel, and 350 μL serum-free media in each of the remaining two channels. For the experiments with netrin-1 being released from fibroblasts, transfected fibroblasts (1×10^5 cells) were seeded in the chemoattractant channel (source), and normal fibroblasts (non-transfected, 1×10^5 cells) were seeded in the left channel (sink). Unless transfected, these normal fibroblasts do not inherently release netrin into the media. Netrin-1 released from the transfected fibroblasts diffuses across the collagen-1 gel and creates a gradient. The medium was changed at regular intervals to maintain chemogradient at all times. The control devices which received no guidance cues were cultured in the same procedure as with test cases.

Characterization of neurite outgrowth and turning

Phase-contrast, fluorescence and confocal microscopy were used to characterize neurite distribution and quantify neurite turning in 3D collagen gels within the devices. Florescent and phase contrast images were acquired with a Nikon TE300 microscope equipped with a Hamamatsu camera and Openlab image acquisition software. Neurite and nuclei staining were performed after fixation with 4 % PFA (30 min). The fixed samples were rinsed thrice with 1X phosphate buffered saline (PBS), treated with 0.1 % Triton-X (1-2 min), rinsed with 1X PBS twice followed by the infusion of a mixture of DAPI (for nuclei) and rhodamine phalloidin (for actin; 30 min) and a final wash step with 1X PBS. The rhodamine phalloidin stains both axons and dendrites within the 3D scaffold. Confocal images were collected using a spinning disk confocal microscope (Zeiss Axiovert 200M) furnished with Imaging Suite (Perkins Elmer Life Science) acquisition software. A series of 20 optical serial sections (5 μm thick) were obtained and the aligned images stacked and rendered for 3D visualization using Imaris (Bitplane, MN). The last 100 μm segment along the length of each neurite leading to the growth cone was traced with NeuronJ[34], and the angle this segment makes with the horizontal line (0°) was measured. Among the four quadrants, values in Q1 (-60° to +60°) reflect growth towards guidance cue and in Q3 (120° to 240°) reflect turning away from the guidance cue (Fig. 6J). The number of neurites in quadrants 1 and 3 were counted for devices cultured under similar conditions, and the statistical significance values between test cases and control cultures (with no guidance cues) were computed using Mann-Whitney test by averaging the data from all the devices under each

experimental condition. For studies with DRGs, the number of cells which migrated into each quadrant were measured and quantified using a similar procedure.

Results and discussion

Microfluidic device implementation

Microfluidic devices offer numerous practical advantages, including high-throughput and low-cost experiments, when compared to traditional gradient-generating techniques. Besides, microfluidic devices require smaller amounts of valuable reagents which allow multiple gradient-generating cell culture environments to be implemented in parallel. The device developed in this study offers a novel platform for studying neurite guidance *in vitro*, and provides many unique features not available in other current techniques: (i) It is easy to fabricate, simple to manipulate, and more reliable in reproducibility of experiments. (ii) The cells can be cultured in more physiological conditions, since they are packed in a tissue-like conformation and project neurites through a 3D matrix (Fig. 5). The good survival and outgrowth from these neurons demonstrates a very effective way to culture these cells in the future. (iii) Chemogradients across the 3D gel can be established at desired time points to study the neurite biology. (iv) With multiple neurites per device and multiple devices per batch, it is possible to obtain statistical significance of data with just one experiment. (v) It is easy to track neurites in 3D and compute turning angles, and therefore conducive to detailed analysis and quantification. In conclusion, we believe that these devices offer an efficient tool for studying neurite guidance in response to chemo-gradients.

The device has a T-shaped gel region and three channels (Fig. 1B): media channel, cell channel and guidance cue channel. As the guidance cue added to the right channel diffuses through the gel, the other channels act as a sink for the same, thereby creating a gradient across the gel. Earlier studies have shown that the initial axonal outgrowth of cortical neurons is predominantly directed laterally, with progressive axonal turning at more lateral positions[35]. Thus, relative to cell body, the gel region was purposefully designed long enough to visualize enhanced neurite outgrowth and eventual turning response to the gradient. The three PDMS posts (Fig. 1C) provide structural support to the gel and prevent gel from overflowing into the media channels prior to gel polymerization, via surface tension forces which dominate at these length scales[36]. Thus, in this configuration, the direction of neurite outgrowth is orthogonal to the direction of gradient, making this an effective setup to study neurite guidance. In addition, when cells must be circulated through a narrow channel, there is an increased risk of damage by shear stress. The chamber in which the cells were cultured was several orders of magnitude larger than the cell body, greatly increasing their chance of survival and reducing their tendency for mechanical activation while introducing them into the device.

Previous studies have demonstrated that cells within 3D scaffolds exist in a more natural environment in which they contact other cells and ECM in three dimensions, and are therefore expected to more closely evoke native cell responses than 2D substrates[37]. Since cellular gene expression within 3D scaffolds (as in native tissues) can be regulated by scaffold-derived cues including cell adhesion molecules, growth factors, and mechanical stimuli, ECM-based scaffolds are more likely to evoke native

integrin-ECM interactions and preserve the native cell phenotype[38]. A reconstituted hydrogel of type I collagen at 2 mg/ml was used in the present study producing a polymerized matrix with fibrils 50-200 nm in diameter, and pore size on the order of 0.5-1 μm[39]. Although this is not the predominant extracellular matrix component in the nervous system, type I collagen has been successfully used by other researchers to study neurite outgrowth in both 2D and 3D cultures[40]. Our preliminary studies also showed no adverse affects of collagen type I on neuron survival and neurite outgrowth, compared to matrigel or peptide gel.

Gradient establishment and stabilization

In preliminary gradient experiments, the chemoattractant was added to the device, and all the other channels were filled with the same volume of serum-free media, in an attempt to create gradient. However, convection through the gel was observed even after equilibrium was attained, probably due to small pressure differences between side channels, which might prevent diffusion gradient from forming across the gel. Thus, to maintain equilibrated pressures in the side channels, a PDMS reservoir system with two sections was installed on top of the device (Supplemental Fig. 1). One section of reservoir filled with chemoattractant (or repellant) medium enclosed the chemoattractant channel port, while the other section filled with media covered the other two channels. A small channel shaped as a half cylinder with diameter 1.5 mm connected these two sections of the reservoir and allowed pressures to equilibrate, thus preserving the gradient through the gel. Fig. 2A shows typical time-dependent snapshots of gradient

obtained with a 40 kDa FITC-Dextran in the device, from which concentration profiles across the gel were obtained over the 2 day period (Fig. 2B). It was observed that the gradient takes 30 min to establish, and a stable gradient could be maintained for up to 2 days. The gradient advanced to the left in the initial 30 min, after which the chemoattractant slowly depleted from the chemoattractant channel around the entrance of the gel, gradually accumulating in the cell and media channels. Deviations from a linear gradient are evident due to the T-shape of the gel region, but these are highly reproducible, can be predicted by the computational model, and can be accounted for in the interpretation of the experiments if necessary.

Recent studies by Goodhill et al., quantified gradient detection by growth cones using both experimental and computational approaches[41,42,43]. The steepness of the gradient was characterized by the change in concentration across the width of growth cone (~10 μm) normalized by the concentration at the source and expressed as a percentage. While gradients as low as 0.1% can be detected by growth cones, a 1% gradient is sufficient to induce some guidance and 10% steepness will induce robust guidance[9]. Since growth cones are exposed to a variety of gradients in their native environment *in vivo*, they likely adapt their morphology and directional guidance depending on the magnitude of the concentration and the gradient[44]. If the concentration is high enough that all the cell surface receptors are saturated, then no amount of gradient will have any effect. On the other hand, if the concentration is too low, very few receptors would be activated despite higher gradients. Thus, it is critical to decouple the effects of concentration levels and gradient on cellular responses to growth factors. Regardless of the perceived distortions (e.g., gel-filling region and the

cell channel acting as sinks) to the maintenance of a uniform linear gradient across the gel in the device, our finite-element modeling predicted a steepness of 3-4 % (data not shown) at the concentrations studied, which should induce robust neurite guidance. Our future studies are geared towards precise measurement of guidance strength, i.e., the difference in receptor activation across the growth cone and axonal shaft, to gain better understanding of axonal response to these guidance cues. To maintain a steeper gradient for extended periods in this device, it would be better to slowly pass media through the side-channels during the experiment. This procedure not only constantly replenishes chemoattractant in the source channel, but also prevents its accumulation in cell and media channels which might act as sinks.

Gradient sensitivity to external perturbations

The role of external perturbations on gradient establishment and stabilization during the experiment were tested in two ways: media change in the device at regular interval, or adding 150 μL of Dextran solution to the chemoattractant reservoir on top of the device. When media is changed in all the channels, the reservoirs and ports are emptied and replaced with fresh media. Concentrations were monitored during media change (Fig. 3A), showing that the higher concentrations from fresh media reestablished the gradient across the gel within ~30 min, after which it remained stable. In a second experiment, 150 μL of dextran solution was added to the chemoattractant reservoir which already contains 350 μL of media. This caused a significant increase in the pressure in this compartment which was effectively equilibrated through the reservoir-connecting

channel, and not through the gel disrupting the gradient (Fig. 3B). Similarly, when the device was moved from incubator (at equilibrium) to microscope for imaging, or when the cells were packed onto the gel surface, or when the incubator itself experienced vibrations, no significant changes in gradient across the gel were observed (data not shown). Thus, these detailed studies show that the gradient was formed with a high degree of certainty in the device, and also recovers well from external perturbations.

Despite these advances, a number of uncontrollable variables may contribute to gradient disruption in cell culture studies. For example, rapid evaporation of media, variation in concentration of collagen gel near PDMS wall or posts, unwashed debris in channels, binding of guidance cues to matrix, etc. Thus, necessary precautions have been taken to autoclave and visually check the devices before use, utilize collagen gel from the same batch, and maintain same collagen gel to neuron ratio for all experiments.

Gradient simulation

The finite element model of the time dependent gradient in the microfluidic device was shown in Fig. 4. The steady state concentration distribution across the gel region in the device (Fig. 4A) and the spatio-temporal evolution of the concentration profiles in this region (Fig. 4B) were calculated. In the initial conditions, the chemoattractant channel has a concentration of 1, and the cell and media channels have concentrations of 0. The concentration gradient (slope of the concentration profile) distribution across the gel region was shown in Fig. 4C for comparison, and its spatiotemporal evolution profile in

Fig. 4D. It can be seen that it takes approximately 30 min for a quasi-steady concentration gradient to be established, which decays slowly within 42 h, after which the chemoattractant and the medium are replenished. Furthermore, the decaying concentration profiles lead to a more uniform gradient within the gel region over time. These results are in excellent agreement with experimental data on diffusion of Dextran across the 3D gel within the device. However, we do not expect to see variation in the concentration profiles of the guidance molecule across the height of the device, since the height of collagen gel in our device (120 μm) is significantly smaller than the gel width (1200 μm). Thus, gradients in chemoattractants will primarily develop in the x-y plane without much variation in the z-plane at each slice, in the gel region of the device. The concentration gradients at two different locations in the 3D gel, parallel to the neurite growth, were simulated to understand the chemogradients experienced by growing axons near and far from the source (Supplemental Figure 2). In conclusion, an exact knowledge of the concentration gradients and the ability to perform detailed parametric studies using simulations are important for quantifying the chemoattractant gradient sensed by the neurite tip to interpret their turning potential.

Effect of chemoattractive gradients on neurite guidance

The goal of the experiment was to make the neurons grow their neurites in three-dimensions into the collagen gel and neurons have a greater chance of doing this if they are close to the gel surface. Therefore, the cells were packed onto the gel by a differential pressure across the gel as shown in Fig. 5. The cell suspension (20 μL) was placed in the inlet port of the cell channel and the media from all the other ports was removed. The high pressure created by the cell droplet will induce flow through the cell

channel towards the outlet port. The low pressure in both the media channel and chemoattractant channel creates a small flow through the gel, thus packing the cells onto the gel surface. By reestablishing the pressure difference several times, the flow was restored, and the cell density packed onto gel increased. The medium was refreshed in the cell channel 2 h after cell seeding to eliminate the unpacked cells.

Netrin-1, a diffusible chemoattractant produced by floor plate cells, plays an important role in creating a complex pattern of neuronal connectivity by facilitating directed migration of immature neurons over long distances. Some studies have shown that netrin-1 mediates outgrowth of commissural axons *in vitro* via DCC receptor[45], and enhances retinal neurite extension[31, 46]. On the other hand, netrin-1 has been shown to be a chemorepellent for oligodendrocyte precursor cells in the embryonic spinal cord, mediated via a netrin-receptor complex consisting of DCC and an UNC-5 homolog (UNC5H)[47]. Thus, in this study, we evaluated the role of netrin-1, delivered through different modes, on hippocampal neurite turning and guidance in microfluidic devices *in vitro*.

When hippocampal neurons were cultured in control devices with no exogenous guidance cues (Fig. 6G), a majority of neurites exhibited random outgrowth and turning in 3D collagen gel in the absence of any gradient, with only 8.3 ± 3.1 % of total neurites observed in Q1 and 12.6 ± 4.3 % in Q3 (n = 151 neurites; Fig. 6K). The neurite turning of neurons cultured with netrin-transfected fibroblasts in the right channel and normal fibroblasts in left channel was shown in Fig. 6A, while the neurite turning in cultures with normal fibroblasts in both the channels was shown in Fig. 6B. Netrin-1 released from netrin-transfected fibroblasts (Fig. 6A) attracted 43.4 ± 6.5 % of total neurites towards

the gradient, with only 7.1 ± 3.9 % turning away ($p < 0.001$ for Q1 vs. Q3; $n = 119$). In contrast, cultures with normal fibroblasts on both sides with no netrin gradient across the gel (Fig. 6B), exhibited no preferential neurite turning ($p > 0.6$ for Q1 vs. Q3; $n = 45$). In the former case, netrin-transfected fibroblasts might be continuously replenishing the gradient across the collagen gel, with the cell and media channels acting as a sink, although the exact concentration of netrin-1 being released from these cells is not known at this point. Netrin-1 release from fibroblasts therefore induced a three-fold increase in neurite turning towards the gradient when compared to non-transfected fibroblast cultures ($p < 0.001$; Fig. 6J), and a 5-fold increase when compared to fibroblast-free controls ($p < 0.001$).

Exogenous supplementation of 1 μg/mL lab-purified netrin-1 encouraged DCC-transfected hippocampal neurite turning towards the gradient (27.8 ± 6 % in Q1; $p < 0.01$ for Q1 vs. Q3; $n = 117$) (Fig. 6C), thrice the percentage of neurites which turned into Q1 in netrin-free controls ($p < 0.001$ vs. controls). The differential effects of lab-purified netrin concentration on neurite response to the gradient were then tested. Fig. 6 (panels D, E, F) shows the representative fluorescent images of hippocampal neurons cultured in the presence of 0.1, 1 and 10 μg/mL netrin, respectively. Quantitative analysis of these images revealed that 0.1 and 10 μg/mL netrin had no significant chemoattractive effect on neurite turning ($n = 138$ and $n = 38$ neurites, respectively), compared to netrin-free controls. Higher concentration of netrin (10 μg/mL) might be saturating the netrin-1 receptors resulting in a loss of neurite response, while 0.1 μg/mL is too low for binding to enough receptors to induce any response[43], which would explain the lack of any positive response at these dosages. In addition, studies have

shown that optimum guidance is obtained when the concentration is on the order of the dissociation constant of the guidance cue and its receptor on the growth cone[43]. However, further studies are needed to calculate the concentration-dependent receptor activation in these cultures and validate these hypotheses. In conclusion, 1 μg/mL netrin offered the maximum positive effect on neurite turning towards the gradient in the dosage range studied ($p < 0.03$ for 1 μg/mL netrin vs. all the other cases).

When hippocampal neuron cultures were supplemented with 0.1 μg/mL brain pulp (Fig. 6H; $n = 28$), a 3-fold increase in neurite turning toward the gradient was observed relative to controls ($p < 0.005$). It was interesting to note that the hippocampal neurons responded in a similar fashion to both 1 μg/mL lab-netrin and 0.1 μg/mL brain pulp, as evident from the percentage of neurites in Q1 and Q3 under both cases (Fig. 6K). Though it is difficult to identify the composition and concentration of each guidance cue in the brain pulp mixture which contributed to this neurite response, it nevertheless shows the utility of this device to culture whole protein isolate from tissue specimens with a known cell type.

The cell culture environment is much more physiological in this device, when compared to 2D flat surface culture systems or the micropipette turning assay. Chemoattractant was added to the device when the growing neurites reach the horizontal section of the gel, where the gradient becomes nearly orthogonal to the direction of neurite growth. The growth cone is extremely dynamic in nature and fulfills three important functions – sense environmental cues, transmit signals to the cell body and navigate the neurites accordingly. Growth cone migration is mediated by the

polymerization/ depolymerization of cytoskeletal elements connected with the actin superstructure, which have been implicated to play a key role in axonal outgrowth, growth cone motility and guidance[48]. Guidance cues were shown to induce chemotropic responses in growth cones *in vitro*, wherein attractive cues such as netrin-1 or BDNF (brain-derived neurotrophic factor) extend the cytoskeletal network in the direction of the gradient[49], and proteins induced by repulsive cues such as slit-2 or semaphorin3A cause it to collapse[50]. Netrin-1 is secreted into the matrix environment and binds to ECM molecules and cell membranes, thereby determining the range of netrin diffusion and signaling[51]. Thus, netrin signaling could be due to activation of different netrin receptors, with DCC (*deleted in colorectal cancer*) receptors primarily mediating netrin attraction[52], and UNC-5 receptors mediating netrin repulsion[53]. Since collagen-1 is not the predominant component of ECM in the nervous system, netrin-1 binding to 3D collagen-1 scaffold will be negligible[26], which will not affect the perceived gradient by neurites in the device. Results from this study also confirm that the hippocampal neurite turning toward the 1 μg/mL netrin-1 gradient is mediated by DCC-receptor activation in the leading edge of growth cone, as shown by the bright fluorescence of DCC receptors in Fig. 6C.

Effect of slit-2 on neurite guidance

Slit-2 has been shown to repel neuronal precursors migrating from the anterior subventricular zone to the olfactory bulb[54], repel spinal motor axons in culture by interacting with Robo receptor[55] and mediate glioma cell guidance in the brain. In

conjunction with their Robo transmembrane receptor counterparts, slit-2 has been shown to regulate guidance of commissural axons at the midline[56]. In addition, cells that are repelled by slit-2 were shown to lose responsiveness towards netrins[57, 58]. In knock-out mice lacking expression of slit-2, severe defects in axonal guidance were observed in vivo[59]. Since slit-2 is a well studied chemorepellant in neurobiology, we evaluated the effects of slit-2 gradient on neurite turning in microfluidic devices.

Fig. 7 shows representative collapsed 3D confocal microscopy images of hippocampal neurite turning at two different levels of slit-2 gradient. At the higher gradient (250 ng/mL in the right channel) slit-2 acted as a strong chemorepellant (Fig. 7A), as evident from the percentage of neurites in Q3 (42.6 ± 9.1 %) compared to that in Q1 (18.2 ± 4.5 %; $p < 0.001$ for Q3 vs. Q1; $n = 64$). In contrast, slit-2 at 62.5 ng/mL did not exhibit similar strong repellent characteristics (Fig. 7B; $n = 51$). Increasing the concentration of slit-2 from 62.5 ng/mL to 250 ng/mL almost tripled the percentage of neurites that turned away from the high concentration ($p < 0.001$; Fig. 7C). Relative to controls which received no cues (Fig. 6G), 250 ng/mL slit-2 enhanced neurite turning down the gradient by 3.4-fold ($p < 0.001$). However, further studies are needed to understand the molecular mechanisms (e.g., receptor activation) behind this interesting behavior of slit-2 on hippocampal neurite turning.

Effect of slit-2 on DRG migration and neurite guidance

When DRG explants were seeded in the cell channel, neurons overpopulated the devices and aggressively migrated into 3D collagen gel (Fig. 8A). In control cultures,

which received no slit-2, neuronal migration into Q1 and Q3 remained similar due to lack of any gradient in the scaffold (18.5 ± 5.1 % in Q1 vs. 15 ± 6.5 % in Q3). On the other hand, 250 ng/mL slit-2 addition drastically increased DRG neuron migration down the gradient (74 ± 12.5 % in Q3; Fig. 8C), by 5-fold relative to controls ($p < 0.001$ vs. controls), and by 2.7-fold relative to 62.5 ng/mL slit-2 gradient ($p < 0.01$). Migrating neurons have been shown to utilize different signaling pathways than chemotaxing growth cones, by extending multiple processes and then selecting the one that appears most favorable for migration[60]. The leading tip of the migrating DRG neurons (Fig. 8A) preceding the cell body supports this strategy adapted under chemogradients. Taken together, these results suggest that slit-2 at 250 ng/mL concentration expresses a strong chemorepellant effect for DRG neuron migration, and further studies are needed to elicit the molecular mechanisms behind these observations.

In order to inhibit DRG cell growth and migration and allow only neurite extension into the collagen scaffold, we added 5-fluorourasil (5-FU, 10^{-5} M concentration, Sigma Aldrich, USA), a pyrimidine analog drug used extensively in cancer research for inhibiting cell migration and proliferation[61]. In these experiments, the DRG explants were seeded in the cell channel along with 5-FU on day 0, and after 24 h culture, all the channels were washed extensively with fresh media to remove traces of 5-FU from the gel. Since no cell migration into the scaffold was observed at this stage, a gradient was established in the devices by adding 250 ng/mL of slit-2 to the right hand channel. Representative fluorescence images show extensive DRG neurite outgrowth and turning in 3D collagen scaffolds (Fig. 8B), cultured in the presence (or absence) of 250 ng/mL slit-2. Quantitative analysis revealed that 70 ± 14.2 % of DRG neurites were

repelled by slit-2, compared to 42 ± 8 % neurites in control cultures ($p < 0.03$ vs. controls). DRG neurite turning into Q1 was significantly inhibited (by 56 %) on slit-2 addition, relative to that in control cultures ($p < 0.05$ vs. controls). These results were in broad agreement with the effects of 250 ng/mL slit-2 on hippocampal neurite turning in this device (Fig. 7).

In addition to its potential in neurobiology studies, this device might also be of use in tissue engineering and regenerative medicine applications. Numerous studies have reported that an injury to the central nervous system (CNS) could drastically alter the cellular gene expression of guidance cues and their receptors[62]. Of particular interest, changes in expression of netrin-1 and its receptors have been identified following an injury to the spinal cord and cerebellum, possibly accounting for regenerative failure of severed axons in these regions[63]. The manipulation of these developmental cues, organization of their complex spatio-temporal gradients, understanding of cell-cell and cell-matrix interactions, and elucidation of the role of multiple guidance factors for the repair of injured CNS in animal experimental models could be a daunting and expensive task. Under these circumstances, it would be advantageous to recreate the cellular microenvironment in a simple inexpensive microfluidic system *in vitro*, and understand the role of each component (ECM molecules, growth factor gradients, mechanical stimuli, inflammatory environment, etc), as a guide to the design of tissue engineering approaches (e.g., peripheral nerve grafts, injectable hydrogels) for effective axonal regeneration and guidance *in vivo*.

Conclusions

A novel microfluidic device was designed, developed and optimized to study neurite guidance under chemo-gradients. The main advantages of this system include simplicity in fabrication and usage, cell culture in a physiological 3D environment, and maintenance of a stable gradient for long duration. Future experiments are underway to maintain constant gradients for even longer times, by continuous flow of media and chemo-attractants though the channels using external pumps. In this study, only known guidance cues such as netrin-1, brain pulp and slit-2 were studied for their influence on hippocampal or DRG neurite turning and DRG neuronal migration *in vitro*. These devices could also be used to screen new guidance molecules, study growth cone morphology, or identify genes involved in axon guidance. Since few methods exist for exposing cells to known gradients *in vitro*, this system could also be used with other cell types to study chemotaxis. Finally, this microfluidic platform can have applications in optimization of biomaterials for neural tissue engineering, studying cancer cell migration, stem cell differentiation into highly specialized neurons, and angiogenesis.

Acknowledgements

The authors would like to acknowledge the early efforts of Ms. Johanna Varner in establishing the microfluidic platform for studying neurons in our lab. Also, funding from an anonymous foundation and device fabrication facilities at Draper Laboratories (Cambridge, MA) are greatly appreciated. Seok Chung was supported by Seoul R&BD program (PA090930).

References

[1] B. J. Dickson, *Science*, 2002, **298**, 1959.

[2] M. Tessier-Lavigne and C. S. Goodman, *Science*, 1996, **274**, 1123.

[3] F. C. Wagner Jr and G. J. Dohrmann, *Surg. Neurol.*, 1975, **3**, 125.

[4] M. B. Bunge, *J. Spinal. Cord. Med.*, 2008, **31**, 262.

[5] G. Curinga and G. M. Smith, *Exp. Neurol.*, 2008, **209**, 333.

[6] D. Mortimer, T. Fothergill, Z. Pujic, L. J. Richards and G. J. Goodhill, *Trends. Neurosci*, 2008, **31**, 90.

[7] H. Chen, Z. G. He, A. Bagri and M. Tessier-Lavigne, *Neuron*, 1998, **21**, 1283.

[8] B. Genc, P. H. Ozdinler, A. E. Mendoza and R. S. Erzurumlu, *PLOS Biology*, 2004, **2**, 2112.

[9] W. J. Rosoff, J. S. Urbach, M. A. Esrick, R. G. McAllister, L. J. Richards and G. J. Goodhill, *Nat. Neurosci.*, 2004, **7**, 678.

[10] S. Lang, A. von Philipsborn, A. Bernard, F. Bonhoeffer and M. Bastmeyer, *Anal. Bioanal. Chem.*, 2007, **390**, 809.

[11] S. Dertinger, X. Jiang, V. Murthy and G. M. Whitesides, *Proc. Natl. Acad. Sci. U. S. A.*, 2002, **99**, 12542.

[12] Z. Pujic, C. Giacomantonio, D. Unni, W. Rosoff and G. Goodhill, *J. Neurosci. Meth.*, 2008, **170,** 220.

[13] J. Q. Zheng, M. Fleder, J. A. Connor and M. M. Poo, *Nature*, 1994, **368**, 140.

[14] K. Buck and J. Zheng, *J. Neurosci.*, 2002, **22**, 9358.

[15] N. Li, A. Tourovskaia and A. Folch, *Crit. Rev. Biomed. Eng.*, 2003, **31**, 423.

[16] J. El-Ali, P. K. Sorger and K. F. Jensen, *Nature*, 2006, **442**, 403.

[17] A. Folch and M. Toner, *Ann. Rev. Biomed. Eng.*, 2000, **2**, 227.

[18] H. Francisco, B. Yellen, D. Halverson, G. Friedman and G. Gallo, *Biomaterials*, 2007, **28**, 3398.

[19] G. Li, J. Lui and D. Hoffman-Kim, *Ann. Biomed. Eng.*, 2008, **36**, 889.

[20] S. S. Margulies, L. E. Thibault and T. A. Gennarelli, *J. Biomech.*, 1990, **23**, 823.

[21] L. J. Millet, M. E. Stewart, R. G. Nuzzo and M. U. Gillette, *Lab Chip*, 2010, **10**, 1525.

[22] A. M. Taylor, M. Blurton-Jones, S. W. Rhee, D. H. Cribbs, C. W. Cotman and N. L. Jeon, *Nat. Methods.*, 2005, **2**, 599.

[23] J. W. Park, B. Vahidi, A. M. Taylor, S. W. Rhee and N. L. Jeon, *Nat. Protoc*, 2006, **1**, 2128.

[24] Y. N. Xia and G. M. Whitesides, *Ann. Rev. Mat. Sci.*, 1998, **28**, 154.

[25] J. C. McDonald, D. C. Duffy, J. R. Anderson, D. T. Chiu, H. Wu, O. J. Schueller and G. M. Whitesides, *Electrophoresis*, 2000, **21**, 27.

[26] M. Yebra, A. M. P. Montgomery, G. R. Diaferia, T. Kaido, S. Silletti, B. Perez, M. L. Just, S. Hildbrand, R. Hurford, E. Florkiewicz, M. Tessier-Lavigne and V. Cirulli, *Developmental Cell*, 2003, **5,** 695.

[27] C. L. Helm, M. E. Fleury, A. H. Zisch, F. Boschetti and M. A. Swartz, *Proc. Natl. Acad. Sci. U. S. A.*, 2005, **102**, 15779.

[28] R. Li, *Methods. Cell. Biol.*, 1998, **57**, 167.

[29] W. E. Thomas, *Life. Sci.*, 1986, **38**, 297.

[30] A. V. Kwiatkowski, D. A. Rubinson, E. W. Dent, J. E. van Veen, J. D. Leslie, J. Zhang, L. M. Mebane, U. Philippar, E. M. Pinheiro, A. A. Burds, R. T. Bronson, S. Mori, R. Fässler and F. B. Gertler, *Neuron*, 2007, **56**, 441.

[31] M. J. Galko and M. Tessier-Lavigne, *Science*, 2000, **289**, 1365.

[32] T. Serafini, T. E. Kennedy, M. J. Galko, C. Mirzayan, T. M. Jessell and M. Tessier-Lavigne, *Cell,* 1994, **78**, 409.

[33] K. Löw, M. Culbertson, F. Bradke, M. Tessier-Lavigne and M. H. Tuszynski, *J. Neurosci.*, 2008, **28**, 1099.

[34] E. Meijering, M. Jacob, J. C. F. Sarria, P. Steiner, H. Hirling and M. Unser, *Cytometry. Part. A*, 2004, **58**, 167.

[35] H. B. M. Uylings, C. G. Van Eden, J. G. Parnavelas and A. Kalsbeek, in *The cerebral cortex of the rat,* ed. B. Kolb, and R. C. Tees, Cambridge, MIT, 1990, p 35-76.

[36] C. P. Huang, J. Lu, H. Seon, A. P. Lee, L. A. Flanagan, H. Y. Kim, A. J. Putnam and N. L. Jeon, *Lab. Chip.*, 2009, **9**, 1740.

[37] W. M. Saltzman, M. R. Parkhurst, P. Parsons-Wingerter and W. H. Zhu, *Ann. N. Y. Acad. Sci.*, 1992, **665**, 259.

[38] L. Griffith and M. Swartz, *Nat. Rev.*, 2006, **7**, 211.

[39] N. Yamamura, R. Sudo, M. Ikeda and K. Tanishita, *Tissue. Eng.*, 2007, **13**, 1443.

[40] G. Li and D. Hoffman-Kim, *Tissue. Eng. Part B.*, 2008, **14**, 33.

[41] G. J. Goodhill, *Trends. Neurosci.,* 1998, **21**, 226.

[42] G. J. Goodhill and J. S. Urbach, *J. Neurobiol.*, 1999, **31**, 230.

[43] J. S. Urbach and G. J. Goodhill, *Neurocomputing*, 1999, **26**, 39.

[44] J. Xu, W. Rosoff, J. S. Urbach and G. J. Goodhill, *Development*, 2005, **132**, 4545.

[45] K. Keino-Masu, M. Masu, L. Hinck, E. D. Leonardo, S. S. Chan, J. G. Culotti and M. Tessier-Lavigne, *Cell*, 1996, **87**, 175.

[46] K. J. Mitchell, J. L. Doyle, T. Serafini, T. E. Kennedy, M. Tessier-Lavigne, C. S. Goodman and B. J. Dickson, *Neuron,* 1996, **17**, 203.

[47] A. A. Jarjour, C. Manitt, S. W. Moore, K. M. Thompson, S. J. Yuh and T. E. Kennedy, *J. Neurosci.*, 2003, **23**, 3735.

[48] D. Bentley and A. Toroian-Raymond, *Nature*, 1986, **323**, 712.

[49] J. Yao, Y. Sasaki, Z. Wen, G. J. Bassell and J. Q. Zheng, *Nat. Neurosci.*, 2006, **9**, 1265.

[50] M. Piper, R. Anderson, A. Dwivedy, C. Weinl, F. van Horck, K. M. Leung, E. Cogill and C. Holt, *Neuron*, 2006, **49**, 215.

[51] T. E. Kennedy, *Biochem. Cell. Biol.,* 2000, **78**, 569.

[52] M. J. Barallobre, M. Pascual, J. A. Del Rio and E. Soriano, *Brain. Res. Rev.,* 2005, **49**, 22.

[53] H. M. Cooper, J. M. Gad and S. L. Keeling, *Clin. Exp. Pharmacol. Physiol.*, 1999, **26**, 749.

[54] W. Wu, K. Wong, J. Chen, Z. Jiang, S. Dupuis, J. Y. Wu and Y. Rao, *Nature,* 1999, **400**, 331.

[55] H. S. Li, J. H. Chen, W. Wu, T. Fagaly, L. Zhou, W. Yuan, S. Dupuis, Z. H. Jiang, W. Nash, C. Gick, D. M. Ornitz, J. Y. Wu and Y. Rao, *Cell*, 1999, **96**, 807.

[56] K. Brose, K. S. Bland, K. H. Wang, D. Arnott, W. Henzel, C. S. Goodman, M. Tessier-Lavigne and T. Kidd, *Cell*, 1999, **96**, 795.

[57] E. Stein and M. Tessier-Lavigne, *Science*, 2001, **291**, 1928.

[58] F. Causeret, F. Danne, F. Ezan, C. Sotelo and E. Bloch-Gallego, *Dev. Biol.*, 2002, **246**, 429.

[59] A. S. Plump, L. Erskine, C. Sabatier, K. Brose, C. J. Epstein, C. S. Goodman, C. A. Mason and M. Tessier-Lavigne, *Neuron*, 2002, **33**, 219.

[60] M. W. Ward, H. Jiang and Y. Rao, *Mol. Cell. Neurosci.*, 2005, **30**, 378.

[61] J. Fried, A. G. Perez, J. M. Doblin and B. D. Clarkson, *Cancer. Res.*, 1981, **41**, 2627.

[62] C. A. Willson, M. Irizarry-Ramirez, H. E. Gaskins, L. Cruz-Orengo, J. D. Figueroa, S. R. Whittemore and J. D. Miranda, *Cell. Transplant.*, 2002, **11**, 229.

[63] R. Wehrle, E. Camand, A. Chedotal, C. Sotelo and I. Dusart, *Eur. J. Neurosci.*, 2005, **22**, 2134.

Figure Captions

Fig. 1. (A) Device fabrication process using soft-lithography technique. SU-8 photoresist spun-coated on silicon wafer (a), and exposed to UV light through a transparency mask (b). PDMS was poured on wafer and cured at 80 ℃ for 2 h (c), and the cross-linked PDMS wafer peeled off (d), ports punched and bonded with cover-slip to close the channels (e). (B) Design of the three-channel microfluidic device developed to study neurite turning in 3D scaffolds under a growth factor gradient. Collagen-1 was injected in the gel-filling channel and allowed to polymerize. The chemo-factor of interest was added to the right channel, basal media added to the left channel to create the gradient, and neurons placed in the cell channel to respond to the gradient (C). The media flow in each channel and the growth factor gradient across the 3D scaffold is also shown (C).

Fig. 2. (A) Time-lapse, normalized images of fluorescent dextran (40 kDa; 10 μM) gradient across the 3D collagen gel in the device. (B) Diffusion profiles analyzed by averaging a horizontal rectangle along the gel region and plotted against its position in the channel. A snapshot of dextran gradient at 24 h time point was shown for reference to origin (0 distance point) in the channel.

Fig. 3. Role of external perturbations on gradient reestablishment in the device. (A) Dextran gradient was completely reestablished in 30 min after media was changed in all

the channels. (B) The steepness of the stable gradient remained unchanged even after the addition of 150 μL of dextran solution to the chemoattractant reservoir.

Fig. 4. Simulation of guidance cue transport in the microfluidic device. The steady-state concentration distribution across the collagen scaffold region after 24 h of guidance cue addition (A) and the concentration gradient (C) in the device; spatio-temporal evolution of the concentration profiles (B) and concentration gradient (D) in these regions plotted along the dashed line shown in (A) and (C), respectively. The reference point for origin (0 distance point) in the channel has also been shown in (A).

Fig. 5. Cell seeding in the microfluidic device. (A) Fluorescent microscopy image of rhodamine-stained neurons attached on glass coverslip in the cell channel before external intervention. (B) A pressure differential created by emptying media channel in the left and chemoattractant channel in the right, resulted in a strong flow through the cell channel and a small flow through the gel, progressively packing cells onto the gel. Fluorescence microscopy image of neurites growing into 3D collagen gel and neurons packed on the surface of the gel, 12 h after seeding.

Fig. 6. Neurite guidance of hippocampal neurons by chemoattractants. Fluorescent images of rhodamine-stained neurons cultured in the presence of netrin-1 released from transfected fibroblasts in right channel and normal fibroblasts in left channel (A), and

normal fibroblasts in both the channels (B). Confocal microscopy images of DCC-transfected neurons cultured with exogenous supplementation of 1 μg/mL lab-purified netrin-1 (C). Confocal microscopy images of rhodamine-stained neurons which received 0.1 μg/mL lab-purified netrin-1 (D), 1 μg/mL lab-purified netrin-1 (E), and 10 μg/mL lab-purified netrin-1 (F), no exogenous supplements (G), and 0.1 μg/mL brain pulp (H). Metrics used for quantification of neurite turning into each quadrant (I), and the percentage of neurites measured in each quadrant in response to external chemoattractive gradients (J and K). Scale bar: images A, B, C, G, H - 100 μm; images D, E, F - 250 μm.

Fig. 7. Dose-dependent effect of slit-2 on hippocampal neurite turning in device. Confocal microscopy images of rhodamine-stained neurons in response to gradient created from slit-2 at 250 ng/mL (A) and 62.5 ng/mL (B). (C) Quantification of neurite turning revealed that 250 ng/mL slit-2 repelled significantly higher number of neurites down the gradient compared to 62.5 ng/mL slit-2 or additive-free controls.

Fig. 8. (A) DRG neuronal (DAPI-stained) migration into 3D collagen scaffold in response to gradients created by 250 ng/mL and 62.5 ng/mL slit-2 in the device. DRG migration in control cultures which received no slit-2 was shown for comparison. (B) Fluorescent microscopy images of extensive DRG neurite outgrowth and turning in response to 250 ng/mL slit-2 and no slit-2 (controls), after neuron migration was inhibited by adding 5-fluorouracil (5-FU) to the culture media. Quantification of DRG

neuron migration (C) and neurite turning (D) into each quadrant, under slit-2 gradient and in control cultures. Significant chemorepellant behavior of 250 ng/mL slit-2 on DRG neuron migration and neurite outgrowth down the gradient was observed relative to controls ($p < 0.001$). Scale bar: images A - 50 μm.

Supplemental Fig. 1. (A) A reservoir cover is added to the top of the device to ensure equalized pressures. The chemoattractant ports are covered with the chemoattractant reservoir (green) and the media and cell channel ports are covers with the media reservoir (blue). A small channel connects both reservoirs to allow differential pressure to equilibrate. (B) A representative confocal 3D image of hippocampal neurite outgrowth in the presence of 0.1 μg/mL brain pulp gradient in the device.

Supplemental Fig. 2. (A) Evaluation of concentration gradient along y-axis using COMSOL. Concentration distribution at steady state with arrows marking the y-axis locations 1 (black) and 2 (green), along which concentration gradients are plotted in (B) and (C), respectively. The concentration gradient values at both locations are normalized with respect to the maximum concentration gradient value at location 1 after 24 h (DC/dx=1), in order to allow for direct quantitative comparison. When chemoattractant is added at t = 0, the concentration gradient at locations 1 and 2 does not exist. However, after 24 h during medium replacement, a stable concentration gradient will have been established.

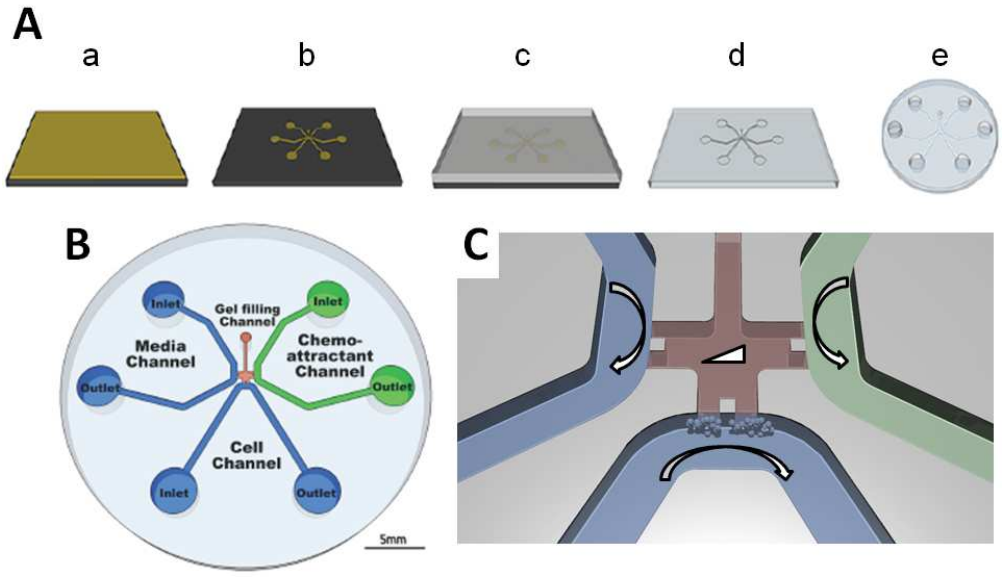

254x149mm (96 x 96 DPI)

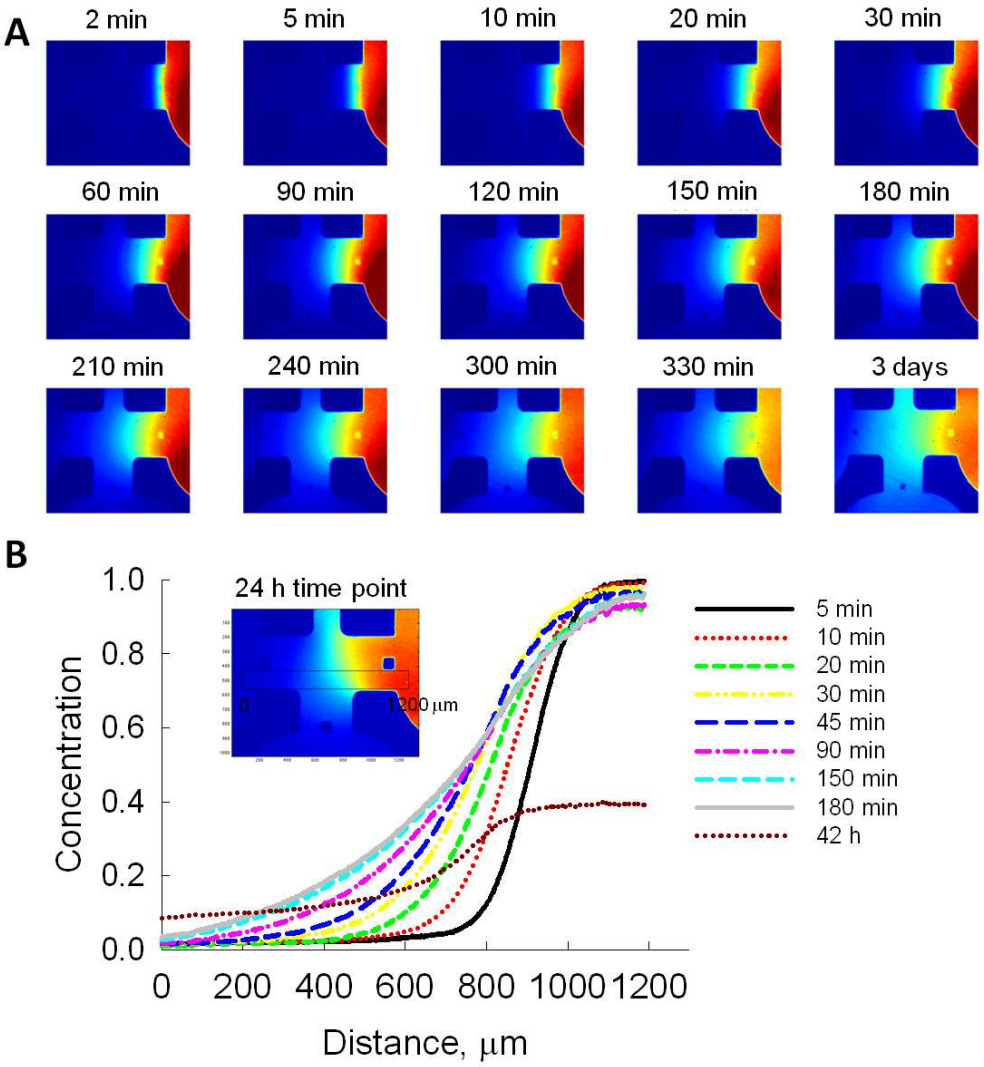

292x317mm (96 x 96 DPI)

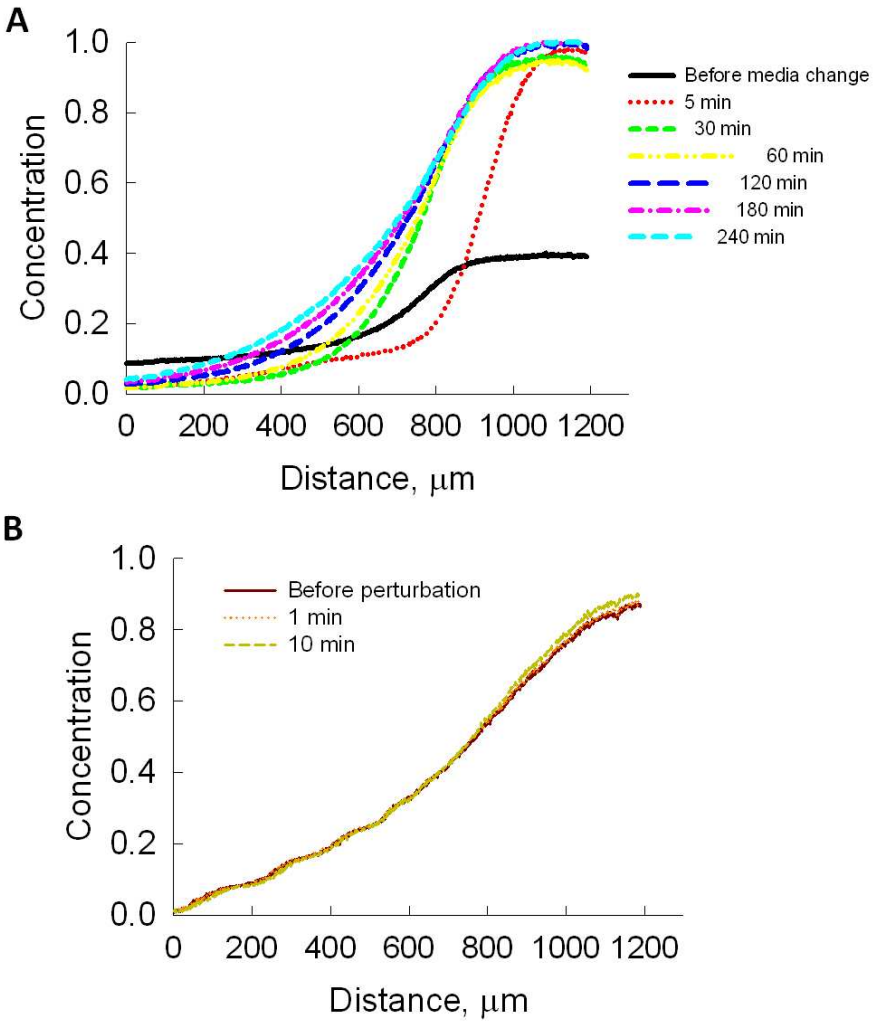

292x304mm (96 x 96 DPI)

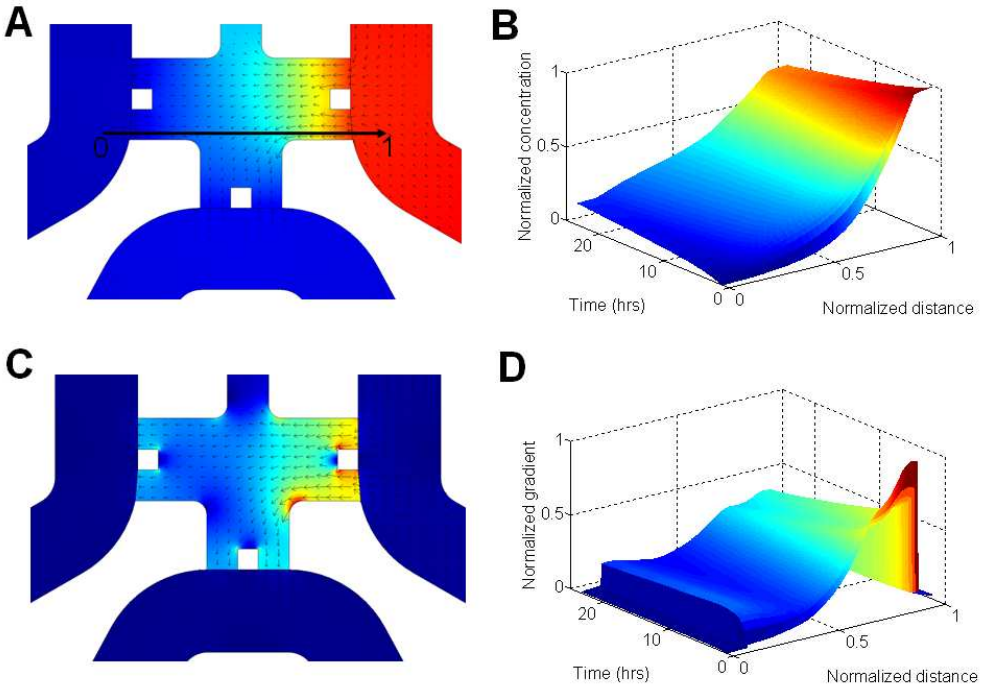

254x190mm (96 x 96 DPI)

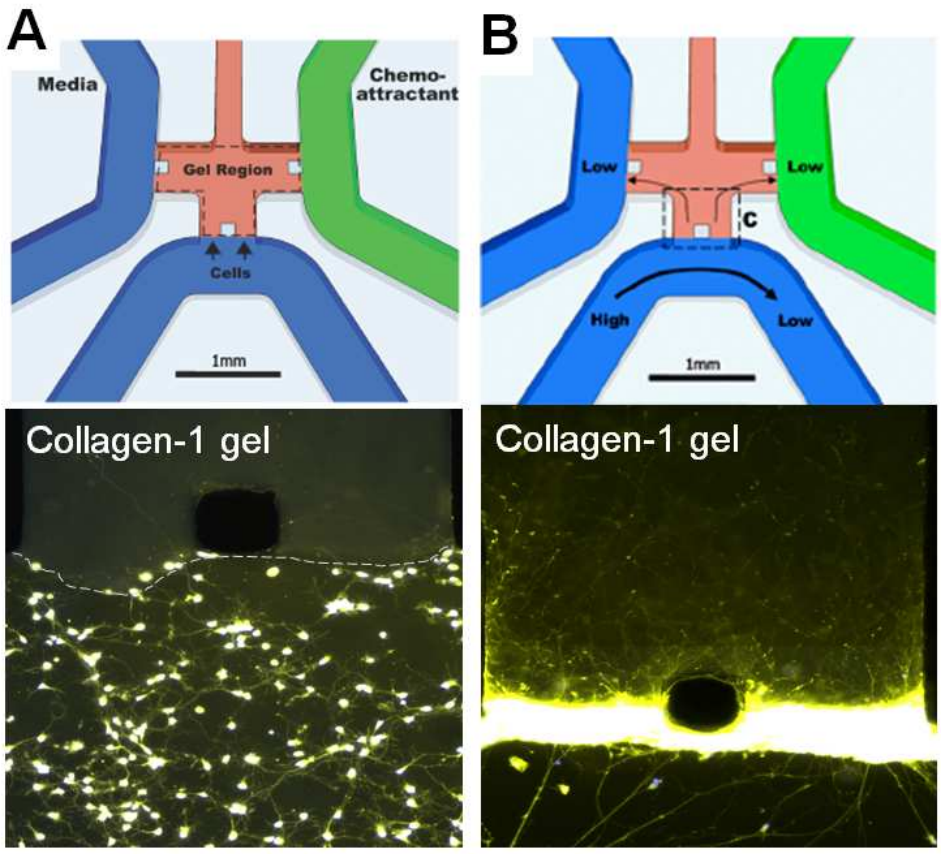

203x177mm (96 x 96 DPI)

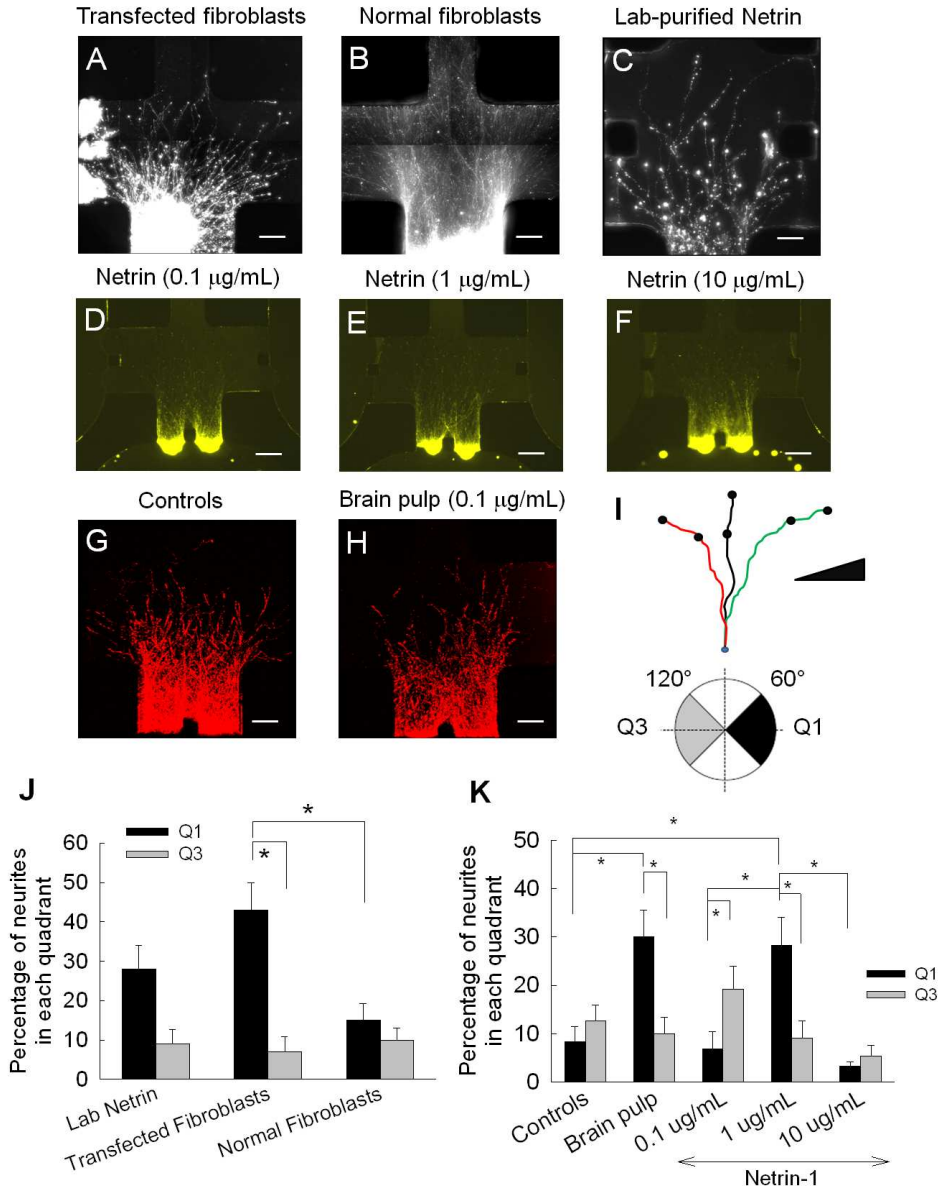

350x441mm (96 x 96 DPI)

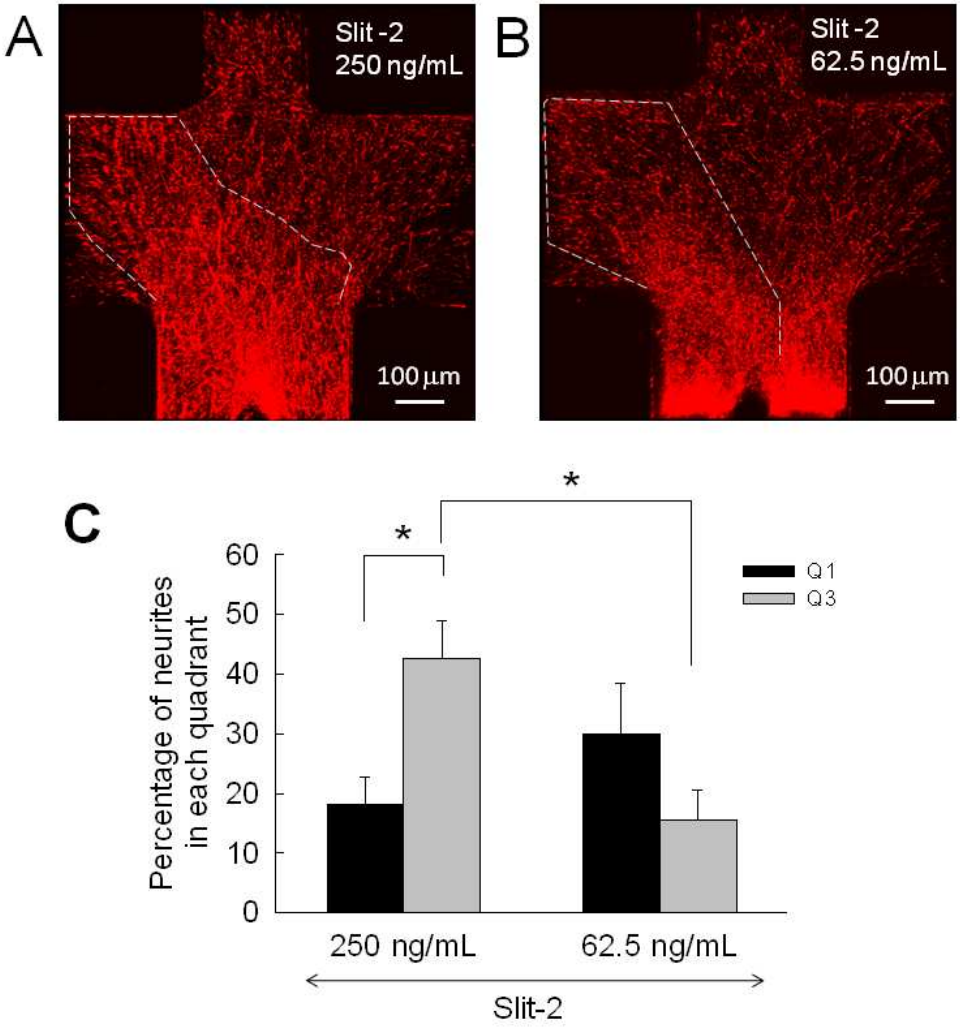

203x215mm (96 x 96 DPI)

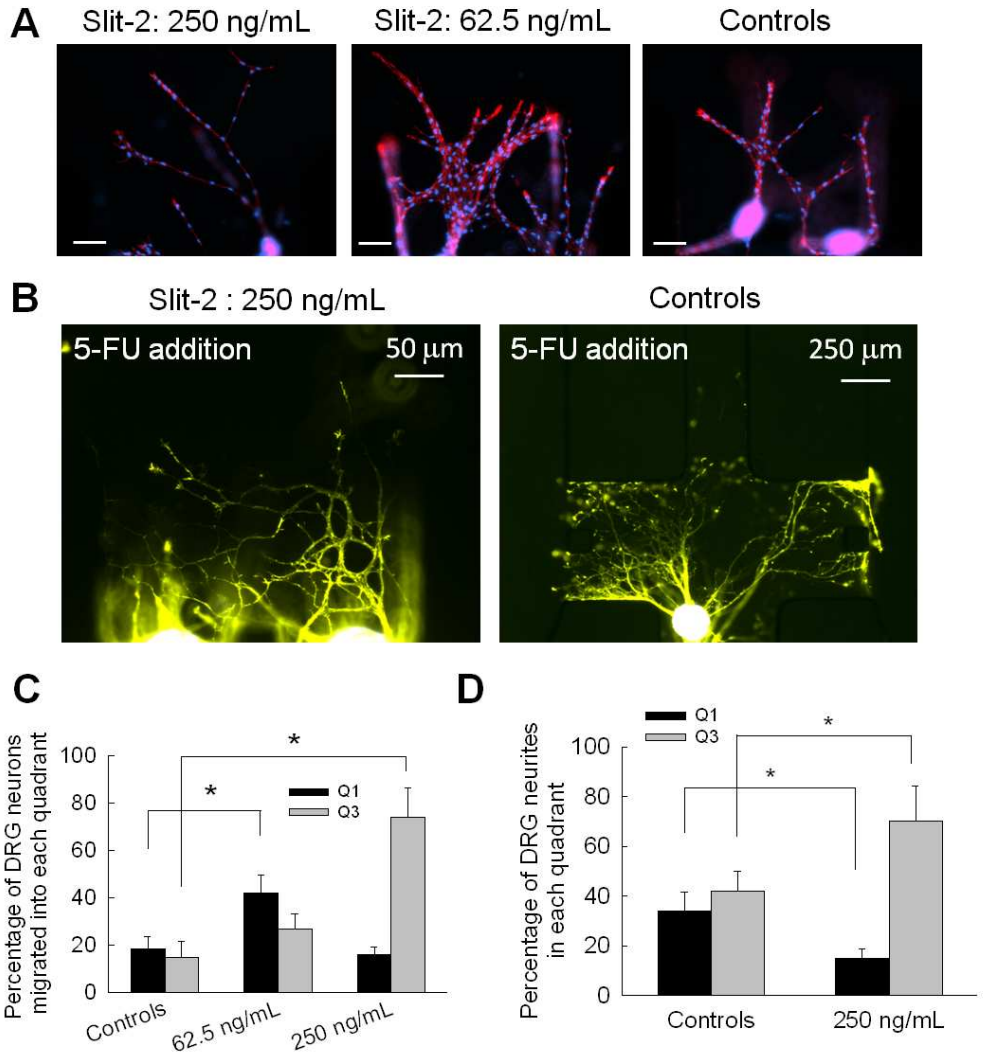

279x304mm (96 x 96 DPI)

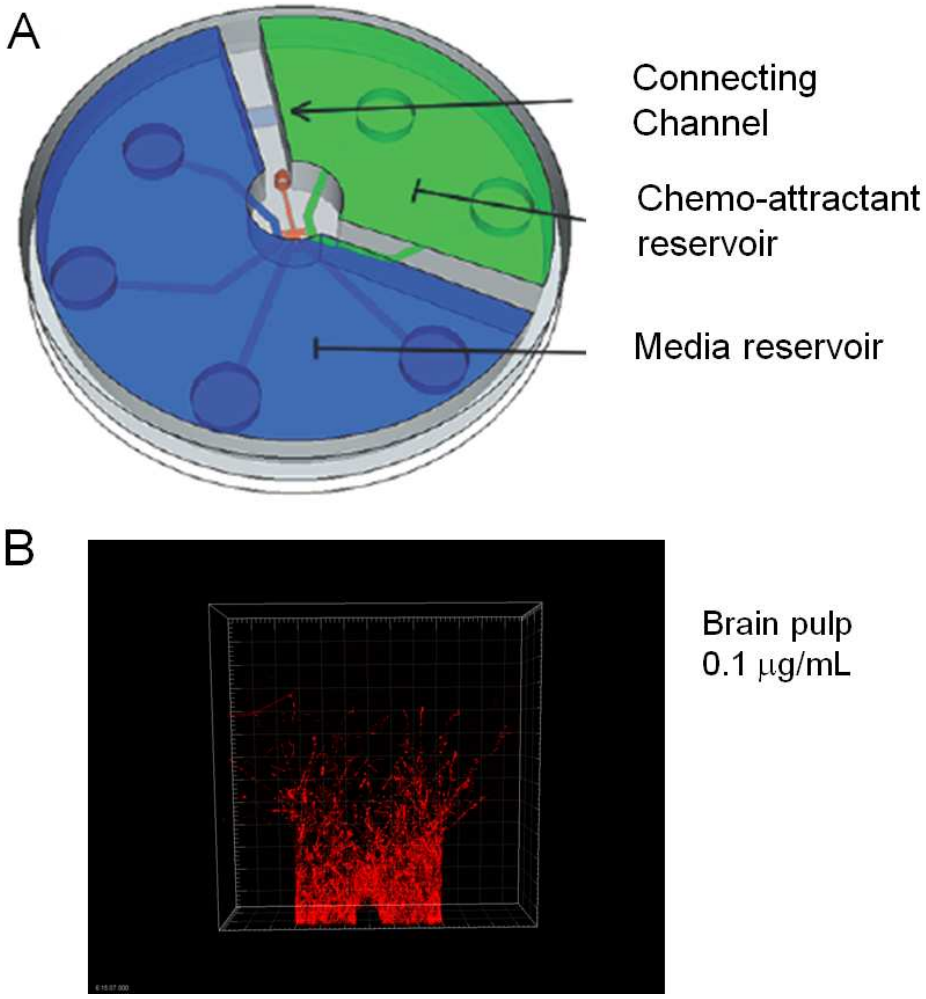

228x228mm (96 x 96 DPI)

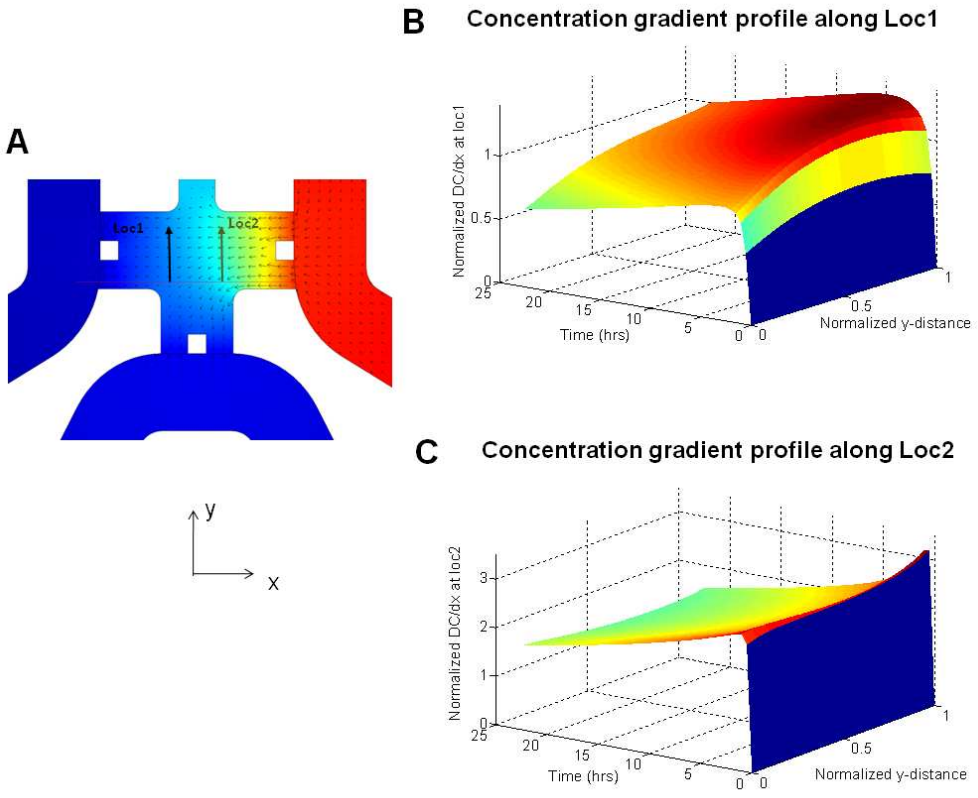

266x223mm (96 x 96 DPI)